

## Core-excited smoothly terminating band in $^{114}\text{Xe}$

E. S. Paul,\* A. J. Boston, H. J. Chantler, and P. J. Nolan

*Oliver Lodge Laboratory, University of Liverpool, Liverpool L69 7ZE, United Kingdom*

M. P. Carpenter, R. V. F. Janssens, F. G. Kondev, and D. Seweryniak

*Physics Division, Argonne National Laboratory, Argonne, Illinois 60439*

C. J. Chiara,† D. B. Fossan, T. Koike, K. Starosta, and D. R. LaFosse

*Department of Physics and Astronomy, State University of New York at Stony Brook, Stony Brook, New York 11794-3800*

A. M. Fletcher, J. C. Lisle, D. Patel, and J. F. Smith

*Schuster Laboratory, University of Manchester, Brunswick Street, Manchester M13 9PL, United Kingdom*

W. Reviol and D. G. Sarantites

*Department of Chemistry, Washington University, St. Louis, Missouri 63130*

R. Wadsworth and A. N. Wilson‡

*Department of Physics, University of York, Heslington, York YO1 5DD, United Kingdom*

I. Ragnarsson

*Department of Mathematical Physics, Lund Institute of Technology, P.O. Box 118, S-22100 Lund, Sweden*

(Received 5 March 2002; published 2 May 2002)

High-spin states have been studied in neutron-deficient  $^{114}_{54}\text{Xe}$ , populated through the  $^{58}\text{Ni}(^{58}\text{Ni},2p)$  fusion-evaporation reaction at 230 MeV. The Gammasphere  $\gamma$ -ray spectrometer has been used in conjunction with the Microball charged-particle detector in order to select evaporation residues of interest. The yrast band has been greatly extended to a tentative spin of  $52\hbar$  and shows features consistent with smooth band termination. This band represents the first evidence for a core-excited (six-particle, two-hole) proton configuration above  $Z = 53$ .

DOI: 10.1103/PhysRevC.65.051308

PACS number(s): 21.10.Re, 23.20.Lv, 27.60.+j

The level structure of neutron-deficient  $^{114}\text{Xe}$  has recently been extended to  $I=27\hbar$  following a low-energy  $^{58}\text{Ni} + ^{58}\text{Ni}$  reaction ( $E_{\text{beam}}=210$  MeV) with a backed target [1]. New results have now been obtained with the Gammasphere  $\gamma$ -ray spectrometer employing this reaction at a higher beam energy ( $E_{\text{beam}}=230$  MeV) and using a thin target to study very high-spin states. As a result, the yrast band in  $^{114}\text{Xe}$  has been greatly extended to  $I\sim 50\hbar$  and the band shows high-spin characteristics of a smoothly terminating structure [2,3]. Comparisons with cranked Nilsson-Strutinsky calculations indicate that at high spin the band is built on a core-excited proton six-particle, two-hole (relative to  $Z=50$ ) deformed configuration involving two  $\pi g_{9/2}$  proton holes that originate from below the spherical  $Z=50$  shell gap. This represents the first evidence for a core-excited ter-

minating band in a xenon isotope ( $Z=54$ ), or indeed in nuclei with  $Z>53$  in this mass region. The  $\pi(g_{9/2})^{-2}$  configuration plays an important role both in mass 110 (until now  $Z\leq 53$ ) terminating bands and in mass 130 superdeformed bands ( $Z=58, 59$ ) [4]. The present results for  $Z=54$  advance the bridge between these two structural features in the two mass regions.

High-spin states in  $^{114}\text{Xe}$  were populated using the  $^{58}\text{Ni}(^{58}\text{Ni},2p\gamma)$  fusion-evaporation reaction, performed at the Argonne National Laboratory, using a 230 MeV  $^{58}\text{Ni}$  beam supplied by the ATLAS superconducting linear accelerator. The beam was incident on two thin self-supporting nickel targets, each of nominal thickness  $500 \mu\text{g}/\text{cm}^2$ . The Gammasphere  $\gamma$ -ray spectrometer [5], containing 101 HPGe detectors, was used in conjunction with the Microball [6] in order to provide exit channel selectivity through determination of the number of evaporated charged particles. In addition, the recoiling evaporation residues were passed through the Argonne Fragment Mass Analyzer (FMA) [7] and were dispersed according to their mass-to-charge ( $A/q$ ) ratio. In the present high-spin analysis of  $^{114}\text{Xe}$ , however, this FMA information was not required.

The Microball charged-particle detector, consisting of 95 closely packed CsI(Tl) scintillators covering 97% of  $4\pi$ , was

\*Electronic address: esp@ns.ph.liv.ac.uk

†Present address: Department of Chemistry, Washington University, St. Louis, MO 63130.

‡Present address: Department of Nuclear Physics, Research School of Physical Sciences and Engineering, Australian National University, Canberra ACT 0200, Australia.

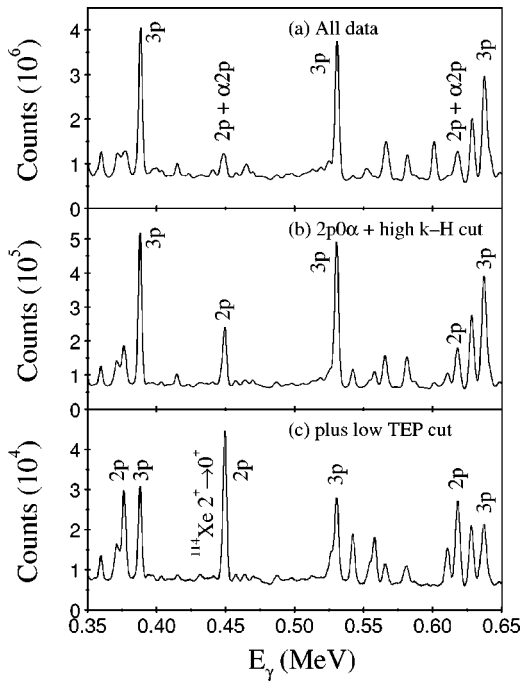


FIG. 1. Singles  $\gamma$ -ray spectra showing enhancement of transitions in  $^{114}\text{Xe}$  ( $2p$  channel) by a combination of charged-particle,  $k$ - $H$ , and TEP gating (see text for details).

used to determine the number of evaporated protons and  $\alpha$  particles associated with an event. Pulse-shape-discrimination and zero-crossover-timing techniques [6] were used to separate light charged particles, including protons and  $\alpha$  particles.

In order to improve the channel selection further, the bismuth-germanate (BGO) anti-Compton shield elements of the Gammasphere spectrometer were used as a  $\gamma$ -ray fold and sum-energy selection device. By removing the Hevimet collimators, the front of the BGO suppression shields were exposed, allowing  $\gamma$  rays to strike the shield elements directly. The number of BGO elements firing and their total energy were recorded for each event providing fold ( $k$ ) and sum-energy ( $H$ ) information. By setting off-line software gates on a two-dimensional  $k$ - $H$  plot, a significant improvement in the quality of the channel selection was achieved; high  $k$  and  $H$  values enhanced the two-particle  $^{114}\text{Xe}$  channel.

Another channel-selection technique consisted in the examination of the  $\gamma$ -ray sum-energy ( $H$ ) recorded by gamma-sphere in relation to the total energy of the charged particles ( $E_M$ ) deposited into the Microball. Off-line gates were placed on a two-dimensional  $H$ - $E_M$  plot (the “total energy plane” (TEP) of Ref. [8]) appropriate for  $^{114}\text{Xe}$ .

Events corresponding to  $2p0\alpha$  evaporation were selected from the original data set of approximately  $6 \times 10^9$  events. In addition, two-dimensional cuts were made on  $k$ - $H$  and  $H$ - $E_M$  plots to enhance the  $^{114}\text{Xe}$  channel. The effect of this selection is illustrated in Fig. 1. The two strongest transitions in  $^{114}\text{Xe}$  ( $2p$  channel) of energies 450 keV and 619 keV are also strong transitions in  $^{110}\text{Te}$  ( $\alpha 2p$ ) [9], which was populated with more intensity than  $^{114}\text{Xe}$  at this beam energy; these transitions are labeled as “ $2p + \alpha 2p$ ” in Fig. 1(a) that

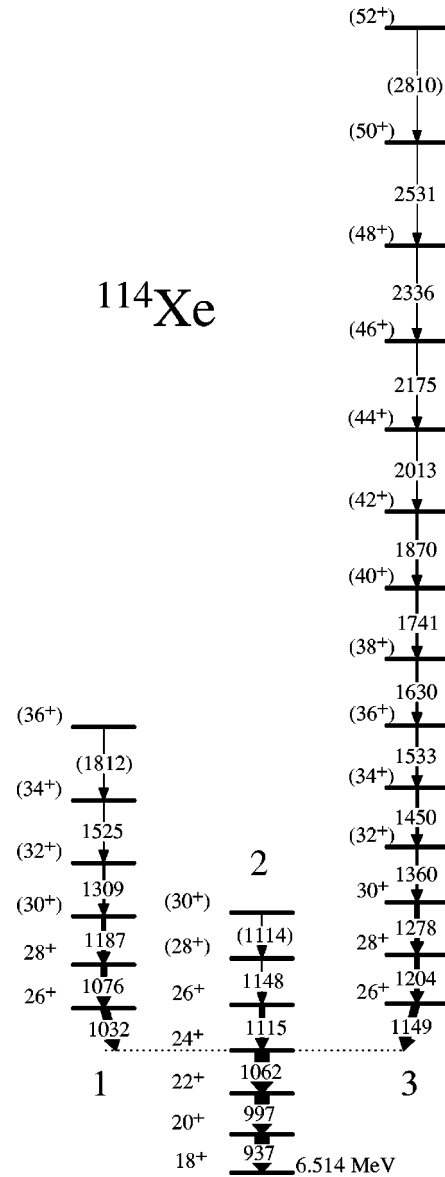


FIG. 2. High-spin positive-parity band structures in  $^{114}\text{Xe}$  with transition energies labeled in keV. Spin assignments up to  $I \sim 30\hbar$  follow from an angular-correlation analysis.

represents the whole data set. Demanding the detection of two protons and high fold/sum energy removes the  $\alpha 2p$  contribution to these peaks in Fig. 1(b). However, considerable  $^{113}\text{I}$  ( $3p$ ) lines are still evident in this spectrum due to the fact that this channel is strong at this beam energy and that there is a  $\sim 30\%$  probability for a proton not being detected in the Microball. The final requirement is to place a cut on the two-dimensional  $H$ - $E_M$  TEP plot, essentially selecting events with high  $\gamma$ -ray sum energy, but low recorded charged-particle (proton) energy. This final cut severely limits the statistics, but greatly improves the  $2p$  lines relative to the contaminant  $3p$  lines, as can be seen in Fig. 1(c). The remaining  $1.2 \times 10^6$   $\gamma$ -ray events, of mean fold 4.6, are, however, sufficient for a high-spin triples ( $\gamma^3$ ) analysis of  $^{114}\text{Xe}$ .

The selected events were unfolded into  $11.5 \times 10^6$  constituent triple ( $\gamma^3$ ) coincidences and replayed into a

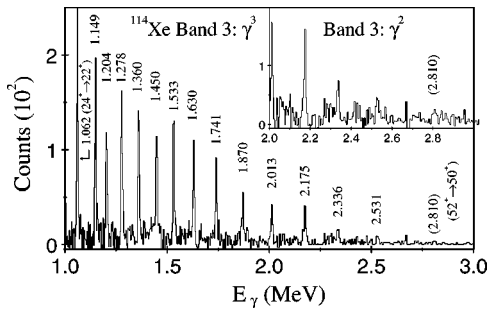


FIG. 3. Triples (main) and doubles (inset)  $\gamma$ -ray spectra for the high-spin yrast band of  $^{114}\text{Xe}$ . Transitions are labeled by their energies in MeV.

RADWARE-format cube [10]. Analysis of the cube was conducted using the LEVIT8R graphical analysis package [10]. These selected events were also used for an angular-correlation analysis. The positive-parity yrast band of  $^{114}\text{Xe}$  has been extended from  $I=24\hbar$  [1] by 14 transitions up to a tentative spin of  $52\hbar$ ; the high-spin level scheme is shown in Fig. 2, while spectra obtained from the cube are displayed in Fig. 3 for the band labeled 3. Another new band of six transitions has been found to feed into the  $24^+$  level and is labeled band 1 in Fig. 2. Finally, the previously known band 2 has been extended by three transitions to  $(30^+)$ .

In order to assign configurations to the high-spin structures in  $^{114}\text{Xe}$ , the energies of the experimental bands are plotted relative to a rigid-rotor reference in Fig. 4 and are compared to theoretical configurations. The calculations,

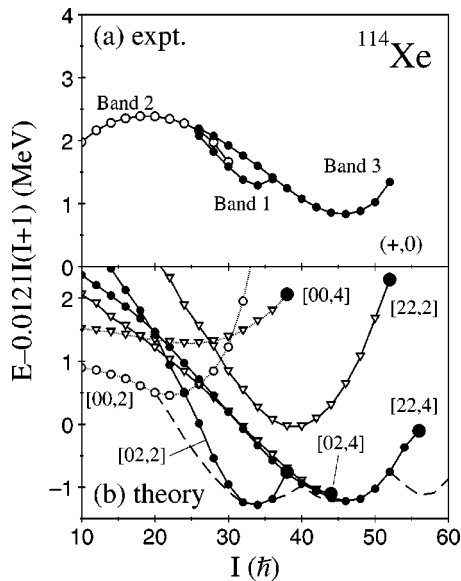


FIG. 4. The energies of the positive-parity experimental bands in  $^{114}\text{Xe}$  at high spin (a), and selected theoretical configurations (b), shown relative to a rigid-rotor reference. The large circles in (b) represent oblate terminating states, while the dashed line follows the locus of theoretical yrast states: a [01,3] configuration for  $I \approx 20-30\hbar$ , a second [01,3] configuration for  $I \approx 36-40\hbar$ , a [12,4] configuration just above  $I=40\hbar$ , and a [23,3(1)] configuration above  $I=52\hbar$ . Note that in the spin range  $30\hbar \leq I \leq 44\hbar$ , the calculated [02,4] and [22,4] curves in (b) are degenerate.

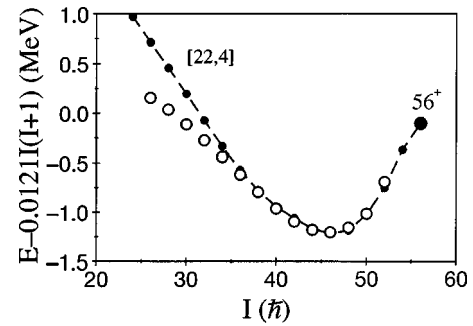


FIG. 5. Comparison of the experimental band 3 (open circles) with the theoretical [22,4] configuration (filled circles) which terminates at  $I^\pi=56^+$ . The data points are normalized at  $I=46\hbar$ .

with constrained orbital occupancy, have been performed using the configuration-dependent shell-correction approach with an unpaired, cranked Nilsson potential, as described in Refs. [2,11,12], and using the Nilsson parameter set of Ref. [13]. The calculated configurations are labeled using the usual  $[p_1p_2, n_1(n_2)]$  nomenclature [12], i.e.,  $p_1$  represents the number of  $\pi g_{9/2}$  holes,  $p_2$  the number of  $\pi h_{11/2}$  particles,  $n_1$  the number of  $\nu h_{11/2}$  particles, and  $n_2$  represents the number of  $\nu i_{13/2}$  particles, relative to the  $Z=N=50$  doubly magic core;  $n_2$  is omitted if equal to zero.

Band 1 is best described by the [02,2] configuration which terminates into an oblate shape at  $I^\pi=38^+$ . Since band 3 is observed to such high spin ( $52\hbar$ ), it clearly must correspond to a core-excited configuration containing two holes in the  $\pi g_{9/2}$  orbital; the lowest-energy configuration predicted by theory is the [22,4] one in Fig. 4(b), which terminates at  $I^\pi=56^+$ , just  $4\hbar$  higher than experiment. Relative to a  $^{100}\text{Sn}$  core, the terminating oblate state may be explicitly written as the  $\pi[(g_{9/2})^{-2}(d_{5/2}g_{7/2})^4(h_{11/2})^2]_{28^+}$  proton configuration coupled to the  $\nu[(d_{5/2}g_{7/2})^6(h_{11/2})^4]_{28^+}$  neutron configuration. The energy minima in the rigid-rotor plots of both bands 1 and 3 agree with those predicted for the [02,2] ( $34^+$ ) and [22,4] ( $46^+$ ) configurations, respectively, reinforcing the confidence in the proposed interpretation.

The rigid-rotor plot for band 3 is compared with that of the theoretical [22,4] configuration in Fig. 5. The experimental and theoretical points are normalized at  $I=46\hbar$ . There is very good agreement for spins  $36-52\hbar$ . Below  $I=36\hbar$ , the experimental points slowly diverge from the theoretical [22,4] configuration that could be caused by a band crossing or an increase in pairing at low spin; pairing is not included in the calculations.

The theoretical shape evolution through the  $\varepsilon_2$ - $\gamma$  deformation plane for several  $(\alpha, \pi)=(0, +)$  configurations in  $^{114}\text{Xe}$  is given in Fig. 6. It can be seen that the [22,4] and [23,3(1)] configurations, including the two  $\pi g_{9/2}$  holes, are much more deformed at low spin ( $\varepsilon_2 \approx 0.30$ ) than the configurations containing no holes. This demonstrates the shape-driving aspect of holes occupying a strongly upsloping “extruder” orbital and also explains the connection between mass 110 terminating bands and mass 130 superdeformed (SD) bands with  $\varepsilon_2 \approx 0.35$ . The latter bands, with a larger valence space, can accommodate more spin before termination is reached, e.g., the yrast SD band in  $^{132}\text{Ce}$  is expected

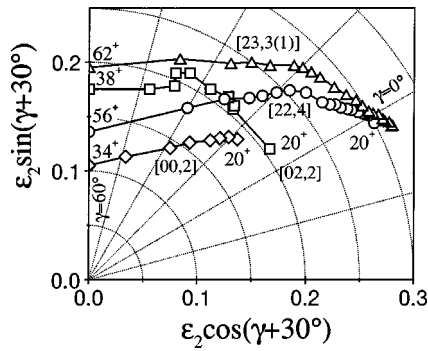


FIG. 6. Theoretical evolution of the nuclear shape for the [00,2] (diamonds), [02,2] (squares), [22,4] (circles), and [23,3(1)] (triangles) configurations in  $^{114}\text{Xe}$ . The data points are separated by  $2\hbar$ .

to terminate at  $I^\pi = 78^+$ ,  $22\hbar$  higher than band 3 in  $^{114}\text{Xe}$ .

Initially, SD nuclei in the mass 130 region were believed to be driven solely by the occupation of  $\nu i_{13/2}$  intruder orbitals from the  $N=6$  oscillator shell [14]. This was consistent with the original observation of a strongly populated (5% of the reaction channel) SD band in  $^{132}\text{Ce}$  ( $N=74$ ) [15,16], while only recently have SD bands been found at or below  $N=72$  [17–19]. The latter work has however shown that the presence of holes in the  $\pi g_{9/2}$  orbital [20] are just as important in forming SD shapes in  $Z\sim 58$  nuclei and that superdeformation still persists as the neutron Fermi surface falls well below the  $N=6$  intruder orbitals. Moreover, Fig. 6 clearly shows a larger quadrupole deformation for the configurations

with two  $\pi g_{9/2}$  holes in  $^{114}\text{Xe}$ ; the configurations with the holes are predicted to possess  $\varepsilon_2 \approx 0.30$  at spin  $20\hbar$ , as opposed to  $\varepsilon_2 \approx 0.20$  for the configurations with no holes.

Band 3 in  $^{114}\text{Xe}$  represents the first evidence for a core-excited smoothly terminating band in this mass region for a nucleus with more than 53 protons. Previously, such structures had been systematically observed in nuclei with  $49 \leq Z \leq 53$  [3]. Indeed, in  $^{113}\text{I}$ , with one proton less than  $^{114}\text{Xe}$ , a similar [22,4] configuration represents the most strongly populated terminating band [21]. Terminating bands have been observed in heavier xenon isotopes, but it has not been possible to definitely prove whether they are built on core-excited configurations, involving the  $\pi g_{9/2}$  holes, or not [22,23]. Lifetime measurements in  $^{119}\text{Xe}$  do, however, favor less-deformed configurations without the  $\pi g_{9/2}$  holes [24].

In summary, the yrast band of  $^{114}\text{Xe}$  has been significantly extended to  $I \approx 50\hbar$  and shows the characteristics of a smoothly terminating structure. Comparison with cranked Nilsson-Strutinsky calculations indicates that this band is based on a core-excited proton configuration involving two  $\pi g_{9/2}$  holes. This represents the first evidence for such a configuration in the xenon isotopes and starts to bridge the gap between mass 110 terminating bands and mass 130 superdeformed bands.

This work was supported in part by the U.K. Engineering and Physical Sciences Research Council, U.S. National Science Foundation, and the Department of Energy, Nuclear Physics Division, under Contract No. W-31-109-ENG-38(ANL). We are indebted to Dr. D. C. Radford for providing the RADWARE analysis codes.

- [1] E.S. Paul *et al.*, Nucl. Phys. **A673**, 31 (2000).
- [2] I. Ragnarsson, V.P. Janzen, D.B. Fossan, N.C. Schmeing, and R. Wadsworth, Phys. Rev. Lett. **74**, 3935 (1995).
- [3] A.V. Afanasjev, D.B. Fossan, G.J. Lane, and I. Ragnarsson, Phys. Rep. **322**, 1 (1999).
- [4] A.V. Afanasjev and I. Ragnarsson, Nucl. Phys. **A608**, 176 (1996).
- [5] I.Y. Lee, Nucl. Phys. **A520**, 641c (1990).
- [6] D.G. Sarantites, P.-F. Hua, M. Devlin, L.G. Sobotka, J. Elson, J.T. Hood, D.R. LaFosse, J.E. Sarantites, and M.R. Maier, Nucl. Instrum. Methods Phys. Res. A **381**, 418 (1996).
- [7] C.N. Davids, B.B. Back, K. Bindra, D.J. Henderson, W. Kutschera, T. Lauritsen, Y. Nagame, P. Sugathan, A.V. Ramayya, and W.B. Walters, Nucl. Instrum. Methods Phys. Res. B **70**, 358 (1992).
- [8] C.E. Svensson *et al.*, Nucl. Instrum. Methods Phys. Res. A **396**, 228 (1997).
- [9] E.S. Paul, H.R. Andrews, T.E. Drake, J. DeGraaf, V.P. Janzen, S. Pilotte, D.C. Radford, and D. Ward, Phys. Rev. C **50**, R534 (1994).
- [10] D.C. Radford, Nucl. Instrum. Methods Phys. Res. A **361**, 297 (1995); **361**, 306 (1995).
- [11] T. Bengtsson and I. Ragnarsson, Nucl. Phys. **A436**, 14 (1985).
- [12] A.V. Afanasjev and I. Ragnarsson, Nucl. Phys. **A591**, 387 (1995).
- [13] J.Y. Zhang, N. Xu, D.B. Fossan, Y. Liang, R. Ma, and E.S. Paul, Phys. Rev. C **39**, 714 (1989).
- [14] R. Wyss, J. Nyberg, A. Johnson, R. Bengtsson, and W. Nazarewicz, Phys. Lett. B **215**, 211 (1988).
- [15] P.J. Nolan, A. Kirwan, D.J.G. Love, A.H. Nelson, D.J. Unwin, and P.J. Twin, J. Phys. G **11**, L17 (1985).
- [16] A.J. Kirwan *et al.*, Phys. Rev. Lett. **58**, 467 (1987).
- [17] A. Galindo-Uribarri *et al.*, Phys. Rev. C **50**, R2655 (1994).
- [18] A. Galindo-Uribarri *et al.*, Phys. Rev. C **54**, R454 (1996).
- [19] T.B. Brown *et al.*, Phys. Rev. C **56**, R1210 (1997).
- [20] A.V. Afanasjev and I. Ragnarsson, Nucl. Phys. **A608**, 176 (1996).
- [21] K. Starosta *et al.*, Phys. Rev. C **64**, 014304 (2001).
- [22] H.C. Scraggs *et al.*, Nucl. Phys. **A640**, 337 (1998).
- [23] E.S. Paul *et al.*, Nucl. Phys. **A644**, 3 (1998).
- [24] H.C. Scraggs *et al.*, in *Experimental Nuclear Physics in Europe*, edited by B. Rubio, M. Lozano, and W. Gelletly, AIP Conf. Proc. No. 495 (AIP, New York, 1999), p. 231.